Available online at www.sciencedirect.com
SCIENCE DIRECT®

Journal of the European Ceramic Society 24 (2004) 565–578

www.elsevier.com/locate/jeurceramsoc

Thermal degradation of an oxide fibre (Nextel 720)/aluminosilicate composite

M.-L. Antti[a,*], E. Lara-Curzio[b], R. Warren[c]

[a]*Division of Engineering Materials, Luleå University of Technology, 97187 Luleå, Sweden*
[b]*Metals and Ceramics Division, Oak Ridge National Laboratory, Oak Ridge, TN 37830-6064, USA*
[c]*Materials Science Group, Division of Innovation, Production and Management, Malmö University, 20506 Malmö, Sweden*

Received 5 January 2002; received in revised form 15 March 2003; accepted 6 April 2003

Abstract

The effect of thermal exposure on the microstructure and tensile stress–strain behaviour has been investigated for composites of woven continuous oxide fibres (Nextel 720) in a porous aluminosilicate matrix. The tensile tests were carried out on straight-sided, centre hole notched plates with 0/90° and ±45° orientations. The as-received material was slightly notch sensitive in that the net section fracture stress decreased somewhat with increasing hole diameter but much less than predicted for an ideally elastic, fully notch-sensitive material. After exposure at 1100 °C and for long time at 1000 °C in air the composite was embrittled. In the 0/90 composite this resulted in a reduced fracture strength, a reduced strain to failure as well as a reduced fracture toughness and damage zone size. After exposure for 100 h at 1100 °C (the most extreme exposure applied) the material also became significantly more notch sensitive and had failure characteristics similar to those of a monolithic ceramic. The ±45 composite was also embrittled which resulted in a reduced strain to failure but an *increase* in fracture strength. Density measurements and observations on the microstructure and fracture surfaces indicated that the embrittlement was due mainly to localised densification of the matrix and an increase in fibre/matrix bonding.

Keywords: Composites; Fibres; Mechanical properties; Nextel fibres; Thermal degradation

1. Introduction

It is now well established that continuous fibre reinforced ceramic composites (CFCCs) can be made to have non-brittle fracture behaviour and improved damage tolerance by introduction of a suitably weak fibre/matrix interface which provides a more favourable path for the extension of matrix cracks than penetrating the fibre. To achieve this an interphase is often coated separately onto the fibres during processing and this involves both an increased production cost as well as an added complexity. It has recently been demonstrated that similar crack-deflecting behaviour can also be achieved by means of a finely distributed porosity in the matrix instead of a separate interphase between matrix and fibres.[1–3] Delamination has been shown to occur in the matrix and the crack deflects into a plane parallel to the loading direction.[1] In particular oxide/oxide CFCCs exploiting this principle attract interest as candidate materials for use in combustors, exhibiting damage tolerance combined with inherent oxidation resistance. Their anticipated ability to operate at higher temperatures than the superalloys used today is expected to lead to an increased efficiency and a reduced need for cooling air, as well as a decreased emission of NO_x gases. The life requirements of the material are high, the aim being several hundred thousand hours at at least 1100 °C.

When designing a structural component, the effect of holes and notches on the mechanical properties is an important practical factor to be taken into consideration. For this reason the mechanical strength of CFCCs has frequently been studied in terms of the notch strength and notch sensitivity. The present work concerns the notch strength behaviour of a commercially available composite consisting of laminated, woven mullite/alumina fibres (Nextel 720) in a porous

* Corresponding author. Tel.: +49-920-492093; fax: +46-920-491084.
E-mail address: marta-lena.antti@mb.luth.se (M.-L. Antti).

0955-2219/03/$ - see front matter © 2003 Elsevier Ltd. All rights reserved.
doi:10.1016/S0955-2219(03)00250-4

aluminosilicate (AS) matrix. The results have been presented in general terms in an earlier study.[4] The focus of this study is the thermal instability of the composite microstructure when exposed to elevated temperatures and in particular how this influences notch strength and notch sensitivity. Both 0°/90° and ±45° orientations were investigated.

In common with polymer matrix composites, carbon matrix composites and several non-oxide CFCCs,[5–8] porous matrix oxide/oxide composites exhibit moderate notch sensitivity.[9–12] For example, centre hole plate samples with 0/90 orientation at room temperature exhibit a moderate decrease in net section strength with increasing hole diameter. The strength falls towards a limiting value for large hole diameters that generally lies between 60 and 80% of the unnotched strength. The relatively good notch tolerance is associated with the development of an extensive zone of damage developing from the hole with increasing load which effectively reduces the stress intensity at the hole. In dense matrix composites the damage consists of multiple tensile cracking of the matrix combined with fibre/matrix debonding. In porous matrix composites, shear damage of the matrix is thought to make a significant contribution.[2,12] Composites with ±45 orientation are notch insensitive.[2,12] Their fracture is dominated by shear failure of the matrix. During the composite fracture process the fibre tows can separate without significant fibre fracture. A function of the fibres is to aid the extension of matrix damage thereby reducing the stress intensity. The nature of the centre hole notch test is discussed in more detail in Section 2.

Reports on the thermal degradation of porous matrix, all-oxide CFCCs are scarce. Levi et al.[2] report, for an alumina fibre (Nextel 610) reinforced mullite/alumina composite, little change in unnotched tensile behaviour after up to 100 h in air at 1200 °C. However, a 2 h exposure at 1300 °C led to reduced fracture stress and reduced strain to failure. The authors attributed this to fibre degradation rather than to changes in the matrix and suggested that the use of the more stable Nextel 720 fibre should lead to improved thermal stability. Jurf and Butner[13] observed a decrease to about 70% unnotched strength of the 0/90 material studied here after 1000 h at 1100 °C. It was suggested that the primary explanation for the loss in strength is matrix densification rather than degradation of fibre strength.[13] Long-term ageing has also been performed by Siemens-Westinghouse.[14] At 1100 °C the unnotched strength after 100 h was reduced by over 25% and after 2600 h by over 55%. A heat-treatment of 3000 h at 1000 °C led to a decrease in strength of about 23%. The suggested explanation of the degradation was embrittlement due to densification of the matrix and possibly a phase change.[14] The present authors are not aware of any earlier reports on the notch strength or notch sensitivity of such composites. However, in a study of edge-notched specimens of a 0/90 Nextel 610/AS composite it was found that the failure mode changed from multiple matrix fracture at room temperature to self-similar crack growth at 950 °C. This change led to a significantly increased notch sensitivity.[11]

Fibre degradation as a possible source of composite degradation should also be considered. Nextel 720 fibres consist of alumina grains with an approximate diameter of 0.1 μm distributed among larger (0.5 μm) mullite grains consisting of many smaller subgrains.[15] Investigations of the response of the fibres to thermal exposure are somewhat conflicting. Deléglise et al.[15] observed significant strength degradation only above 1400 °C for 5 h exposure times while Milz et al.[16] observed severe degradation after 2 h at 1300 °C. Petry and Mah[17] report a small loss in strength after exposure for 2 h at 1100 °C. The causes of degradation are also not clear; surface grooving, structural coarsening[17] and local impurity enrichment have been suggested.[16] The conflicting observations could as well be due to differences in the fibre batches used as to experimental differences.

2. The notch sensitivity test

As already indicated the main objective of the present study was to investigate the degradation at high temperatures of oxide/oxide, porous matrix composites and in particular through its effect on the notch sensitivity measured in terms of the tensile properties of centre hole panels. This form of notch sensitivity test, though of practical relevance, is somewhat complex in interpretation. In an isotropic, elastically deforming solid, the maximum stress intensification at the edge of a circular notch in an infinitely wide plate loaded in uniaxial tension is a factor of three regardless of hole size.[18] Thus the strength of an ideally, fully notch sensitive material will be reduced by a factor of three when such a notch is introduced. A fully notch insensitive material will not be weakened since the stress intensification will be dissipated, for example, by plastic deformation. In reality most materials, including long-fibre reinforced composites, exhibit intermediate behaviour leading to a moderate loss of strength that is generally dependent on hole size. The dependence on hole size arises because the circular notch affects and interacts with the material in its immediate vicinity, thereby altering the distribution of the stress intensification; the volume of affected material scales with the hole size.[18] An added complication in experimental situations is that the stress intensification of a circular hole is affected by the width of the tested plate, decreasing from a factor of three to a factor of two as the ratio of hole size to plate width (a/w) approaches 1,[19] thus necessitating a finite width correction. It is also to be noted that the stress intensification

is altered to some extent by anisotropy of elastic properties.[20]

A monolithic ceramic might be expected to be close to an ideally notch sensitive material. However, here the measured strength will depend on the interaction of the stress field around the hole with the flaw population in the material thus again introducing a notch size effect. Moreover, for such brittle solids the quantitative assessment of notch sensitivity is somewhat impractical since a unique value of the notch-free strength is difficult to determine due to the stochastic nature of their fracture stress.

A number of semi-empirical models have been proposed to describe the notch sensitivity of long fibre, laminate composites including the effective crack model proposed by Waddoups et al.,[21] the point stress model[22] and the average stress model.[22] Primarily developed for polymer matrix composites they have also proved applicable to long fibre reinforced ceramics. Above all they can be used to predict the effect of hole size on the basis of a limited number of experimental measurements in combination with fitting procedures. More recently, more physically realistic models based on crack bridging mechanisms have been presented which also successfully predict the effects of notch geometry.[23] However, application of these models requires knowledge of the bridging forces, which usually implies additional experimental measurement.

In the present work the results have been interpreted in terms of the Waddoups approach, not only because of its relative computational convenience but also because it was considered to be appropriate for the composite degraded by heat treatment which was assumed to have become embrittled making measurement of an unnotched strength difficult.

3. Experimental details

3.1. Material

The material studied was a commercially available composite (Composite Optics, Inc, San Diego, USA) consisting of Nextel 720 fibres in a porous aluminosilicate matrix in the form of 3 mm thick plates. The plates consisted of 12 0°/90° woven layers, with a density of 2.6 g/cm^3 and a fibre volume of approximately 48%. The fibre fabric is infiltrated with the matrix in a sol-gel process. After drying with a so-called vacuum-bag technique under low pressure and low temperature, the composite is pressureless sintered.[13] Intermediate re-infiltration of pyrolysis steps are not necessary. The matrix in these types of composites is characterised by a porosity level around 30–40%[10] which renders the matrix sufficiently weak to enable damage tolerance during loading. Test specimens of two different fibre lay-ups (0/90° and ±45°) were produced from rectangular plates of 300×300 mm. Specimens with 0/90 fibre orientation were obtained from two plates (A and B) processed in different batches; ±45° specimens were taken from a third plate (C).

The composites were plain weave with a unit cell of approximately 1200×900 microns (Fig. 1). The warp and weft fibre tows had average widths of 250 and 340 microns, respectively. Furthermore, they exhibited up to 0.5° deviation from the nominal orientation with respect to the side of the test bars in both the 0/90 and ±45° samples.

3.2. Experimental procedure

Tensile tests were performed on centre circular notched straight-sided specimens with a length of 100 mm for tests at ambient temperature and 200 mm for tests at high-temperature. Their width was 12.5 mm. The circular centre hole with its axis normal to the LW surface (Fig. 2) was drilled with a carbide drill. The ratio between hole diameter and specimen width (a/w) was one of three nominal values (0.1, 0.25 and 0.4). For practical reasons the actual values sometimes deviated somewhat from the nominal.

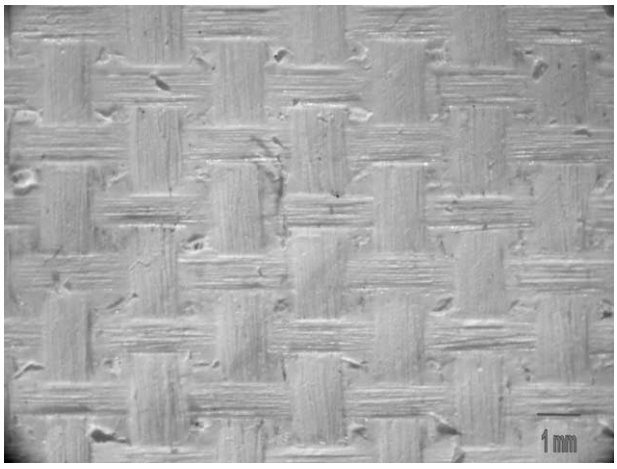

Fig. 1. Fibre fabric structure of the composites. Loading direction ↔.

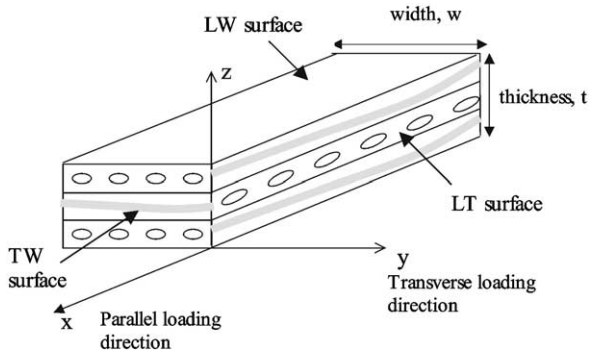

Fig. 2. Definition of test bar surfaces.

Specimens were heat-treated in a box furnace at temperatures of 500, 1000 and 1100 °C for times between 20 and 3240 h. The holes were drilled before heat-treatment but the dimensions used for the stress calculation were measured afterwards. Both as-processed and thermally exposed test specimens were tensile tested either at room or elevated temperature using a servohydraulic mechanical testing machine (MTS 810, Eden Prairie, MN, USA) equipped with hydraulically actuated grips and a compact furnace with SiC heating elements. The tensile tests were performed at a constant cross-head displacement rate of 10 μm/s while the deformation of the specimen was measured over a 25 mm gauge section using a strain gauge extensometer at ambient temperatures, and a low-contact force capacitance extensometer at elevated temperatures.

The tested specimens were embedded in epoxy, polished and examined using optical and scanning electron microscopy (SEM), along axes both transverse and parallel (LT and TW surfaces) to the loading direction (see the schematic diagram, Fig. 2). The fracture surfaces of both fibre orientations were studied in the SEM, both directly and embedded in epoxy and polished on the LW surface. Density and porosity measurements were performed using the Archimedes method as well as image analysis. The microhardness of the matrix was investigated as a function of heat-treatment time and temperature, using a digital microhardness indenter (Matsuzawa MXT-α) at a load of 100 g and a loading time of 15 s.

Test specimens before and after thermal exposure were investigated with X-ray diffraction (XRD). The X-ray spectra were obtained between 10 and 90° 2θ in step intervals of 0.03 2θ at a rate of 1.5 s/step. An automatic divergence slit was used with a beam area of 12×16 mm which thus covered both matrix and fibre regions of the composite. High-temperature XRD has also been performed on pure Nextel 720 fibres, in a powder X-ray diffractometer (Philips PW 1710) with a step of 0.03 2θ at a rate of 8 s/step.[24] After crushing the fibres to a powder heating cycles up to 1400 °C were performed with a heating rate of 5 °C per minute and holding times of 10 min every 150 °C to perform appropriate angular scans.

Selected samples were also examined using Raman spectroscopy. A Dilor XY 800 triple stage Raman microprobe (JY, Inc, Edison, NJ) and an Innova 308C Argon ion laser (Coherent, Inc., Santa Clara, CA, USA) operating at 514.5 nm with a 300 mW output power were used to record Raman spectra from the fibres and the matrix separately. The laser was focused onto areas of interest with an optical objective providing a spatial resolution of ~2 μm.

Table 1
Properties of 0/90 fibre orientation

Sample	a/W	Net-section strength [MPa]	Full section stiffness [GPa]	Hardness HV	Strain to failure [%]
As-received A (RT)	0.10	201	72	–	0.34
	0.26	203	70		0.28
	0.39	197	62		0.26
As-received B (RT)	0.10	204	68	204	0.34
	0.30	179	62.5		0.28
	0.42	191	54		0.29
200 h at 500 °C (B)	0.10	203[a]	74	–	0.32
	0.29	191	62		0.29
100 h at 1000 °C (B)	0.10	180	72	213	0.28
	0.29	172	66		0.24
	0.42	149	57		0.19
3240 h at 1000 °C (B)	0.10	114	80	323	0.15
	0.29	107	74		0.12
	0.42	102	66		0.11
20 h at 1100 °C (A)	0.11	125	81	334	0.17
	0.25	113	73		0.15
	0.39	114	69		0.12
100 h at 1100 °C (A)s	0.10	54.5	90	457	0.06
	0.24	37	83		0.04
	0.38	39	74		0.04
As-rec test at 1000 °C (B)	0.09	210	68	–	0.35
	0.29	171	61		0.24
	0.40	186	56		0.24
As-rec test at 1100 °C (A)	0.09	189	57	–	0.35
	0.24	164	63		0.24
	0.38	154	53		0.18

[a] Failed at grips.

4. Results

4.1. Stress–strain behaviour

Tables 1 and 2 summarise the tensile strength, stiffness, strain to failure and matrix hardness values of the tested samples for 0/90 and ±45 orientation, respectively. Each set of tensile bars contained a replicate samples to assess reproducibility. This was found to be satisfactory.

Representative sets of stress–strain curves for samples with a width of 12.5 mm and an a/w ratio of 0.25 are shown in Fig. 3 (0/90 fibre orientation) and Fig. 4 (±45° fibre orientation). It can be seen that the material with 0/90 fibre orientation lost some strength when heat-treated at 1000 °C; after 100 hours at 1100 °C the strength fell to less than one third of the as-received strength. The 0/90 material lost stiffness when tested at 1100 °C, but after heat-treatment the stiffness at room temperature increased. The strain to failure of the samples with 0/90 fibre orientation was severely decreased after heat-treatment indicating embrittlement of the material.

The ±45° material *increased* in strength after heat-treatment, but the fracture sequences were abrupt and violent compared to the as-received fracture which was a gradual process, indicating an embrittlement after heat-treatment. The stiffness also increased significantly as a result of heat-treatment. It is to be noted that with thermal exposure the properties of the 0/90 and ±45

Table 2
Properties of ±45° fibre orientation (plate C)

Sample	a/w	Net-section strength [MPa]	Stiffness [GPa]	Strain to failure [%]
As-received (RT)	0.10	64	57	0.28
	0.24	61	52	0.19
	0.43	69	47	0.16
200 h at 500 °C	0.10	61	53	0.25
	0.29	64.5	51	0.17
100 h at 1000 °C	0.09	66.5	56.5	0.24
	0.29	66	57	0.14
	0.40	62.5	49	0.15
3240 h at 1000 °C	0.10	91	62	0.27
	0.29	91	63	0.16
	0.40	96.5	58	0.17
100 h at 1100 °C	0.10	94	69	0.25
	0.29	93.5	66	0.16
	0.40	87	56	0.15
As-rec test at 1000 °C	0.10	68[a]	48	0.20
	0.30	81[a]	45	0.22
	0.40	95	40	0.41

[a] Failed at grips, because plate C was not perfectly flat which induced bending forces when clamped.

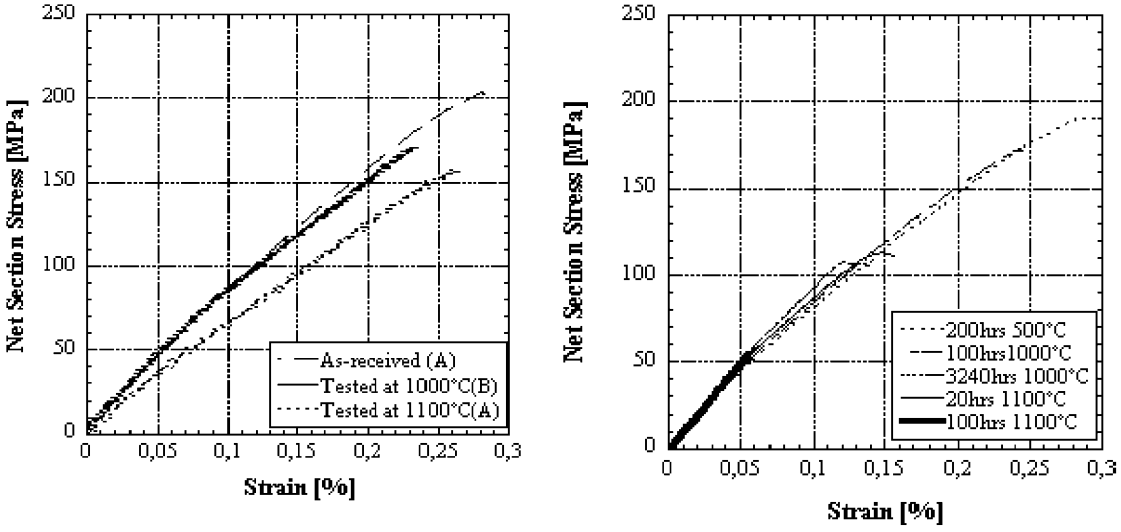

Fig. 3. Representative stress–strain curves of 0/90 samples.

materials approach each other. Most remarkable was the large increase in strength of the ±45 material, with a corresponding increase in strain to failure when tested at 1000 °C.

Whereas the 0/90 samples fractured by fibre bundle fracture and pull-out (Fig. 5 a), the samples with ±45° fibre orientation fractured with little or no indication of bundle fracture (Fig. 5 b). The fracture is presumably able to occur by matrix failure followed by ply separation.

The 0/90 stress–strain curves exhibited a relatively distinct fall in slope (knee) situated in the room-temperature tests at a net stress level of between 30 and 50 MPa and a strain of between 0.03 and 0.06%. This net stress level corresponded to a theoretical intensified stress at the hole of 70–135 MPa. Interestingly, the knee stress and strain were somewhat higher at 1000 and 1100 °C (60–90 MPa and 0.07–0.15%, respectively). The knee is associated with damage in the composite. Fig. 6 shows the stress–strain curve of a load-cycled sample (taken from a parallel study of load cycling)[25] which indicates that the knee is associated partly with a reduction in stiffness and partly with an irreversible strain increment. Indication of shear strain damage occurring diagonally from the hole in the 0/90 composites prior to failure was provided by a parallel study using thermal emission[25] but also here by diagonal, stepped fracture paths in which individual fibre bundles failed in a tensile mode but away from the centre plane of the sample (Fig. 5a).

In Fig. 7 the effect of the heat-treatments on strength are presented in the form of a Larson–Miller plot. For treatments above 500 °C the results (for a given a/w) follow a uniform trend which makes it possible to predict strength values for heat-treatments at other times and/or temperatures. The values from Jurf and Butner,[13] also included in the figure show good agreement with the present results. A minor difference is seen for higher temperatures and/or times, where the material in

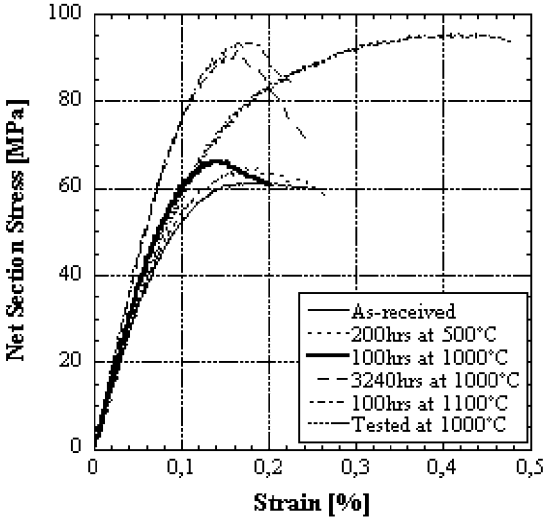

Fig. 4. Representative stress–strain curves of ±45° samples.

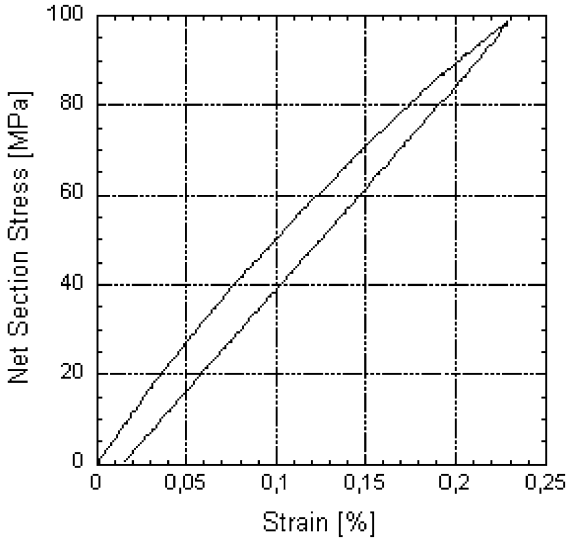

Fig. 6. Stress–strain curve of a load-cycled sample.

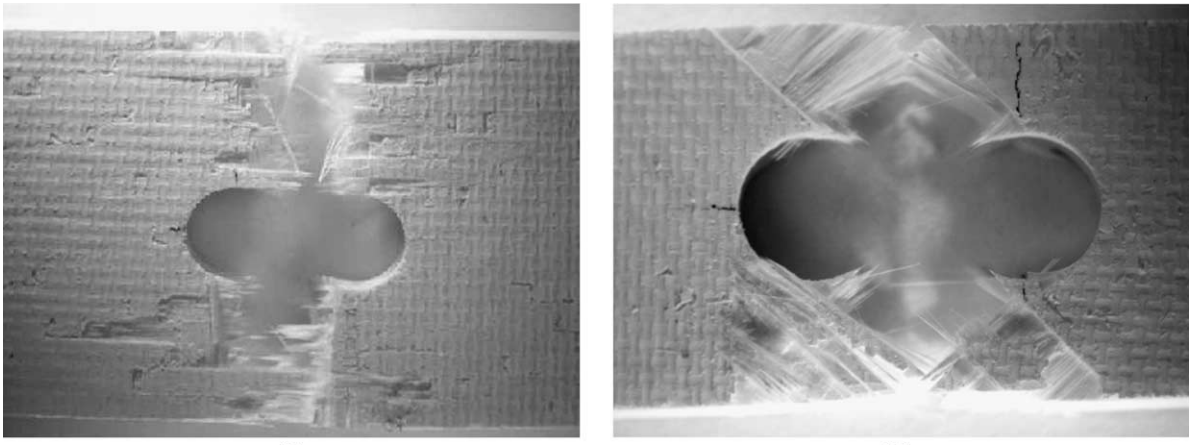

(a) (b)

Fig. 5. As-received samples after tensile testing, showing extensive fibre bundle pull-out. (a) 0/90 fibre orientation; (b) ±45° fibre orientation.

this study shows a larger decrease in strength. This can at least partly be explained by the fact that Jurf and Butner reported unnotched strength.

4.2. Notch sensitivity

As indicated earlier, the tensile fracture stress results for the 0/90 materials were analysed in terms of the Waddoups model. The basis of the model is that the fracture stress, σ_F, of a centre-hole notched infinite plate is given by:

$$K_c = \sigma_F \sqrt{\pi\left(\frac{a}{2} + c_0\right)} \quad (1)$$

where a is the hole diameter, K_c is a critical stress intensity factor and c_0 is the length of each of two cracks on opposite sides of and adjacent to the hole.[19] In fibre composites it is assumed that the cracks are equivalent to the damage zones adjacent to the holes. It is also assumed that both K_c and c_0 are constants, that is independent of hole size, for a given material. The two parameters cannot readily be related to actual physical processes in the material but provided that they are found experimentally to indeed be constants then they offer a convenient means of comparing materials as well as providing a means of strength prediction via Eq. (1). Thus the embrittlement of a composite can be expected to lead to a reduction of both K_c and c_0.

In order to apply Eq. (1) to the present strength values, these were first orrected for the finite width effect by applying the factor $K/3$, where K is the stress intensity factor for a hole in a plate with finite width:[19]

$$K = 3.00 - 3.13\left(\frac{a}{w}\right) + 3.66\left(\frac{a}{w}\right)^2 - 1.53\left(\frac{a}{w}\right)^3 \quad (2)$$

The corrected stress value is in effect the predicted strength of an infinite plate. The width-corrected values for a nominal a/w = 0.25 are listed in Table 3 and for all a/w they are presented in Fig. 8.

The corrected values were used with Eq. (1) to find the K_c and c_0 values for each treatment condition. The three a/w geometries for each condition permitted three independent solutions for these constants. In almost all cases the values obtained lay very close to each other thus justifying the assumption that they were constant within the range of the experiments. Average values for the various heat treatments are included in Table 3 together with the unnotched strength values estimated by inserting the values of the constants into Eq. (1) with

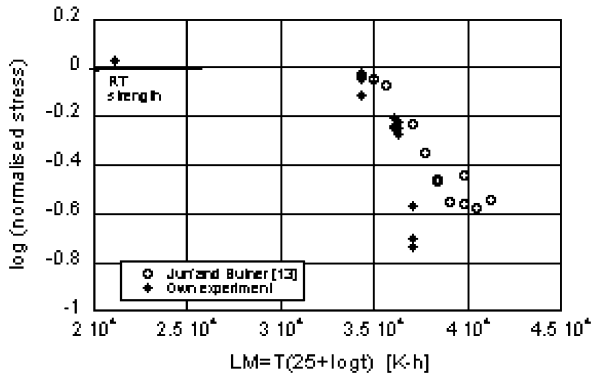

Fig. 7. Larson–Miller plot of strength of heat-treated samples, including literature data.[13] The results are normalised with respect to room temperature strength.

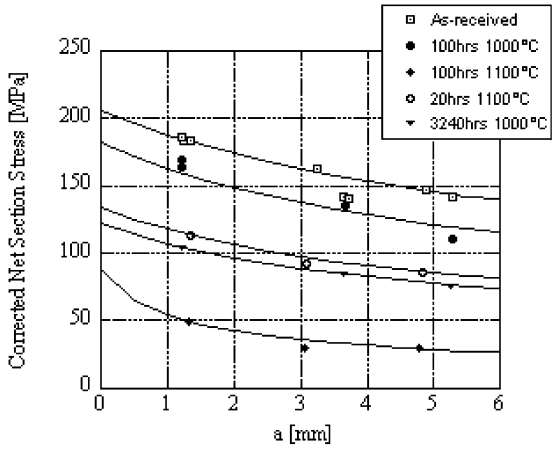

Fig. 8. Net section strength, corrected for finite width, versus hole diameter for 0/90 fibre orientation.

Table 3
Strength values corrected for finite width, and the results of the application of Waddoups model[21]

Sample	Corrected net-section strength[a] [MPa]	K_C [MPa$\sqrt{m}$]	c_0 [mm]	Estimated unnotched strength [MPa]
Fibre orientation: 0/90°				
As-received A (RT)	163	18.9	2.7	205
As-received B (RT)	140	17.5	2.2	210
200 h at 500 °C (B)	–	–	–	–
100 h at 1000 °C (B)	135	14.4	2.0	182
3240 h at 1000 °C (B)	84	8.9	1.7	122
20 h at 1100 °C (A)	92	9.8	1.7	134
100 h at 1100 °C (A)	30	2.7	0.3	88

[a] For nominal a/w = 0.25.

$a=0$. It is seen that the constants indicate a significant embrittlement with increasing treatment time and temperature. The embrittlement is particularly noticeable at 1100 °C, 100 h. This is seen, not only in the low values of K_c and c_0 but also as a greater notch sensitivity measured as the relative loss in fracture strength of notched samples with respect to the unnotched strength. At a/w $=0.25$ the loss was 65% for the 1100 °C/100h material compared with 20–30% for the other treatments and the as-received material.

The constants can in association with Eq. (1) be used to predict the effect of notch diameter on the strength of an infinite plate and these predictions are included as the curves in Fig. 8. The closeness of these curves to the experimental results provides another justification of the applicability of the model.

4.3. Microstructure and fractography

Fig. 9 shows representative micrographs of the fractured, as-received 0/90 material. There were numerous cracks in the matrix perpendicular to the plies (Fig. 9a) one example being shown more closely in Fig. 9b. These never penetrated the fibres. Since the density of cracks was similar in untested material it is supposed that the majority are shrinkage cracks formed during production rather than multiple matrix cracking generated during loading. The shrinkage cracks widened significantly during heat-treatment, probably due to shrinkage of the matrix (see later). There were large voids in some of the fibre-free areas, but also occasionally inside bundles. These large voids will in the following be denoted macropores. The infiltration into most bundles was effective,

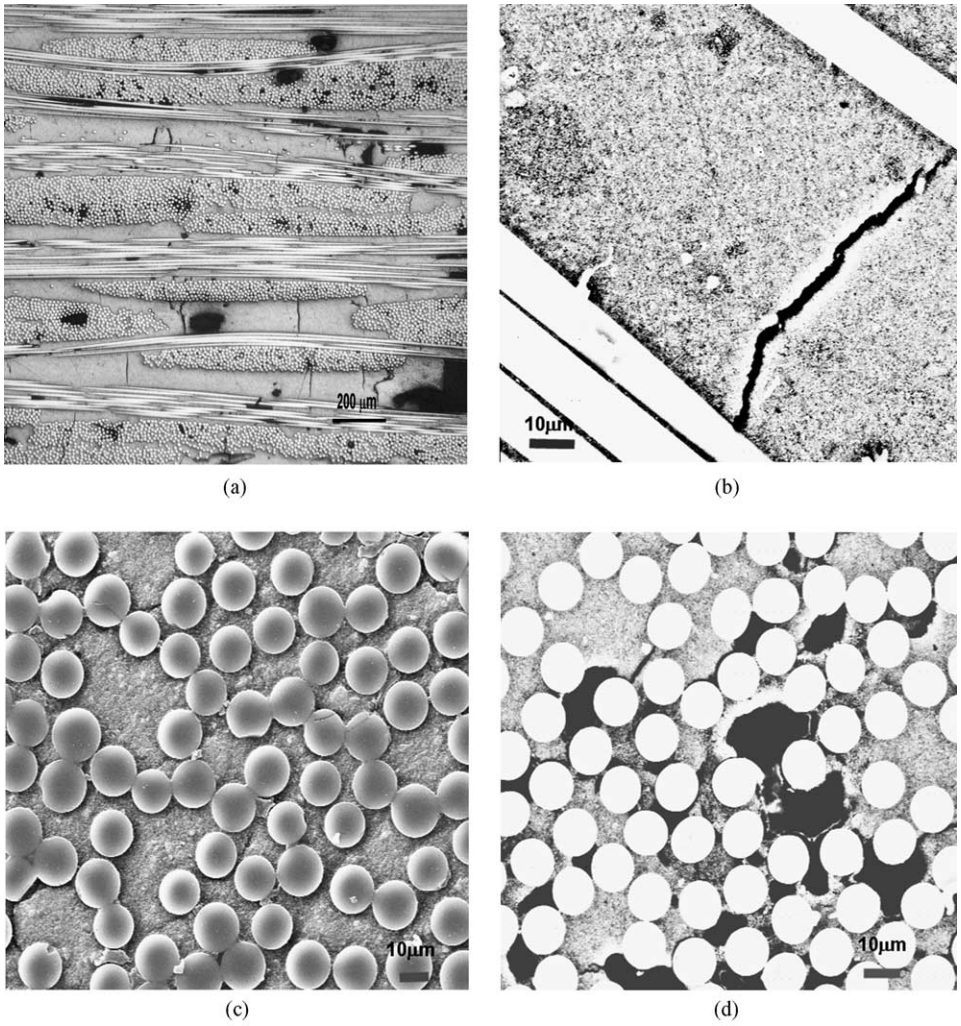

Fig. 9. As-received material showing shrinkage cracks, and voids (a and b) and examples of complete (c) and incomplete (d) bundle infiltration. TW surfaces. (a) Overview, optical microscope. (b) Shrinkage crack between two fibres. (SEM, SEI). (c) Successful infiltration in fibre bundle. (SEM, SEI). (d) Infiltration not complete. (SEM, BEI).

but some of them showed incomplete infiltration (see Fig. 9c and d).

Overviews of the microstructure after heat-treatment for 100 h at 1000 and 1100 °C are shown in Figs. 10a and b, respectively. The heat-treatment caused an opening of some of the shrinkage cracks and coarsening of the macropores. Characterisation of the porosity is presented in Section 4.4. No fibre bundle fractures were found. The response of ±45° material was identical to that of the 0/90 material.

Evidence for shear damage was sought on micrographs of the LW surfaces of fractured samples of as-received 0/90 material. Damage in the form of crack networks in the matrix that could well be attributed to shear deformation was observed in zones stretching diagonally from the holes in several samples.

SEM fractographs of selected fracture surfaces of 0/90 samples are shown in Fig. 11. The as-received material exhibited considerable fibre pull-out. The pulled out fibres were smooth and free of attached matrix consistent with a low ratio of interface debonding energy to fibre fracture energy. After heat-treatment at 1000 °C, fibre pull-out was still extensive but significantly reduced in comparison with that of the as-received material. Moreover traces of matrix material sticking to fibre surfaces could be observed as well as groups of fibres sintered together. Evidence of increased matrix sticking could also be seen in the samples tested at high temperature (i.e. after very short thermal exposure). After heat-treatment for 100 h at 1100 °C the material exhibited negligible fibre pull-out (Fig. 11 c). Very short pull-out of sintered bundles could be found (Fig. 11 d).

The fracture surface of the ±45° material and after heat-treatment for 100 h at 1100 °C is shown in Fig. 12. As mentioned above, at room temperature the samples separated without bundle breakage, failing by inter-laminar shear of the matrix (Fig. 5b). After heat-treatment bundle fracture occurred with no fibre bundle pull-out giving a brittle impression (Fig. 12).

4.4. Density and porosity measurements

The density, porosity and microhardness measurements are summarised in Table 4. The overall dimensions and the weight of the samples and consequently their overall density did not change significantly with thermal exposure. Similarly no significant change in the open porosity was detected. However, there was a significant change in the nature of the macroporosity; the macropores tended to grow larger and some matrix cracks opened during exposure (cf. Figs. 9, 10a and b). The macroporosity was therefore characterised quantitatively on TW sections, defining macropores as all pores with a diameter larger than 22 μm or, in the case of elongated pores and cracks, lengths greater than 44 μm. It was found (Table 4) that the volume fraction of macropores increased with thermal exposure and at 1100 °C their average size also increased. An obvious interpretation of these results is that the matrix densified by sintering. Instead of leading to overall shrinkage of the composite which was constrained dimensionally by the fibre skeleton, the densification occurred internally by growth of existing macropores and matrix cracks. SEM observation did indicate a reduction in the microporosity in the matrix from about 30 to 10 vol.% but

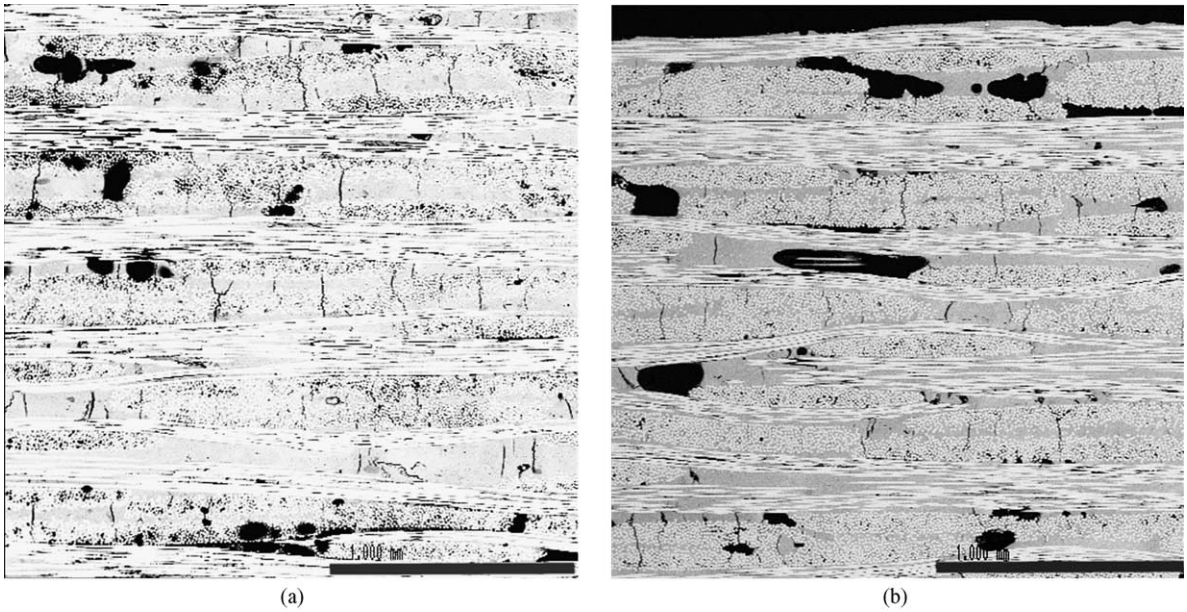

(a) (b)

Fig. 10. Microstructures of material heat-treated for 100 h at temperatures of 1000 °C (a) and 1100 °C (b), respectively (LT surface sections of 0/90° samples). (a) After 100 h at 1000 °C. (b) After 100 h at 1100 °C.

this was not possible to confirm with accuracy due the extreme fineness of the pores. Densification of the matrix was however indicated by an increase in microhardness.

The microhardness of the matrix increased markedly with treatment temperature and time at 1000 and 1100 °C (see Table 4). At a few locations on samples treated at 1100 °C and at 1000 °C for 3240 h very low hardness values were obtained in association with a glassy appearance of the matrix and with the formation of cracks from the corners and edges of the indent. Since SEM–EDS analysis of these locations did not indicate any significant deviation in chemical composition it is possible that large voids lay just beneath the surface in these cases. In Table 4 are listed average hardnesses and standard deviations based on 10 indentations omitting these extremely low values. The scatter of the values also increased significantly after thermal exposure, indicating that the matrix became inhomogeneous. This is also indicated in the micrograph in Fig. 13 where variations in porosity levels can be seen, the denser areas giving brighter reflection. Several indentations also indicated matrix embrittlement after heat treatment by the formation of indentation cracks emanating from indent corners (Fig. 14). It can be noted that the cracks only propagate perpendicular to the fibres and not

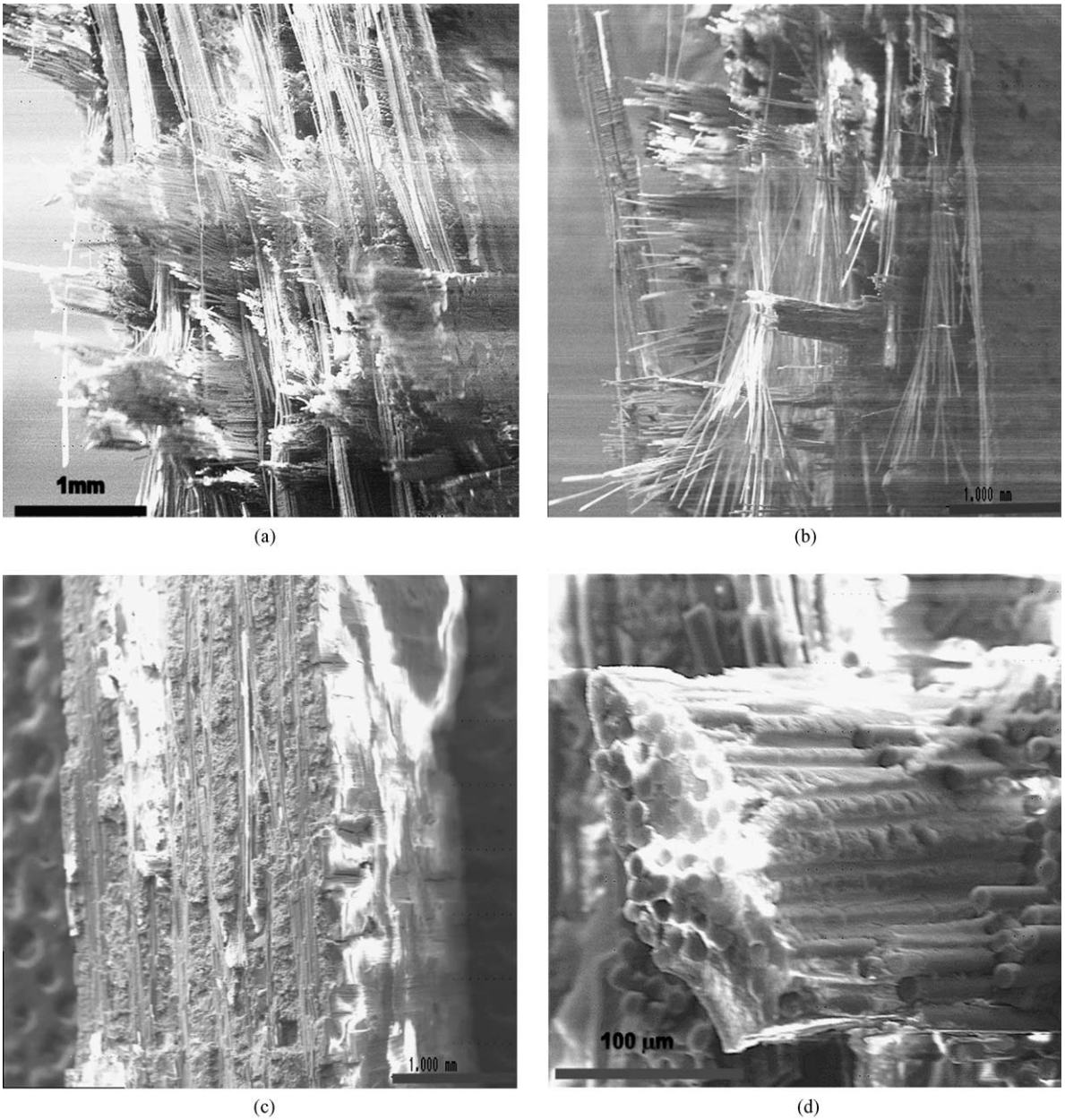

(a) (b) (c) (d)

Fig. 11. Fracture surfaces of as-received and heat-treated samples. (a) As-received. (b) Heat-treated 100 h at 1000 °C. (c) Heat-treated 100 h at 1100 °C. (d) Heat-treated 100 h at 1100 °C showing sintered bundle.

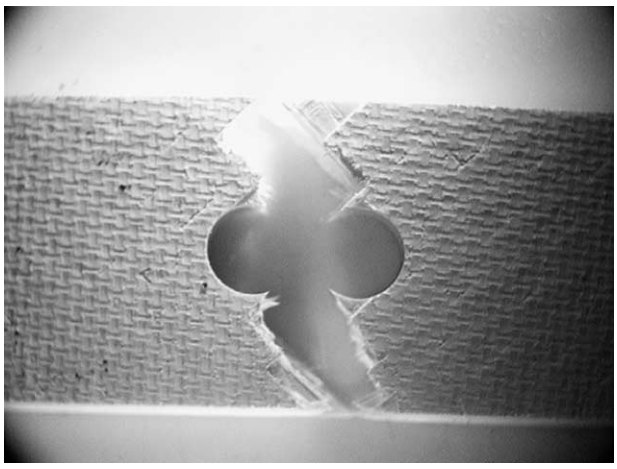

Fig. 12. Fracture surfaces of samples with ±45° fibre orientation after 100 h heat-treatment at 1100 °C.

parallel which is evidence of the constraint imposed on matrix shrinkage mentioned above since such constraint would lead to a tensile stress parallel to the fibres.

4.5. XRD and Raman spectroscopy

X-ray diffraction of the as-received material revealed corundum and mullite peaks and a broad background peak indicative of a glassy phase. The sample exposed at 1100 °C for 100 h, still exhibited mullite and corundum peaks but the background peak had disappeared and peaks corresponding to cristobalite had appeared. It was also observed that the (120) and (210) mullite peaks had shifted somewhat. These observations suggest that the silica in the matrix, originally in the amorphous state, was either already partly segregated or segregated during thermal exposure and then crystallised to cristobalite.

Table 4
Density, open porosity, average pore area and hardness values of the matrix as a function of heat-treatment time and temperature

Sample	Density [g/cm^3]		Open porosity [%]		Average hardness[a] [HV]	Porosity [vol%]	Pores per unit area
	0/90°	±45°	0/90°	±45°			
As-received	2.64	2.68	21.8	20.9	204 (22)	4.3	11.0
100 h at 1000 °C	2.60	2.67	23.2	20.9	213 (54)	–	–
3240 h at 1000 °C	2.64	2.67	22.7	20.7	323 (22)	5.3	14.0
20 h at 1100 °C	2.61	–	22.3	–	334 (33)	6.6	16.4
100 h at 1100 °C	2.64	2.62	22.8	21.8	457 (116)	8.1	13.6

[a] Standard deviations in parentheses. Average taken of 10 indents.

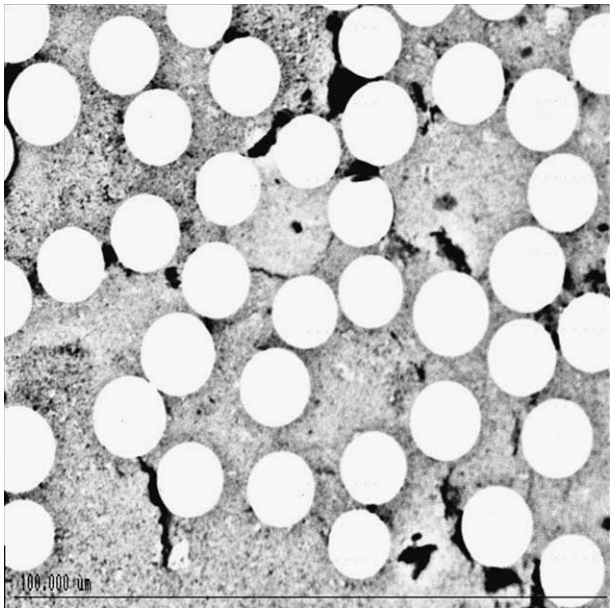

Fig. 13. Inhomogeneous matrix, after heat-treatment 100 h at 1100 °C. LT surface. (SEM, BEI).

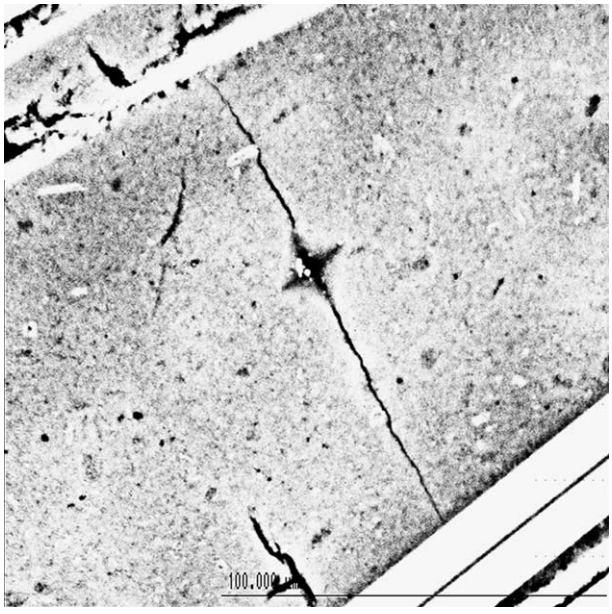

Fig. 14. Indentation cracking after heat-treatment 20 h at 1100 °C. LT surface (SEM, BEI).

These changes were not observed for shorter times at 1100 °C or in a sample exposed for 8 h at 1200 °C.

The results of the HT-XRD study of as-received Nextel 720 fibres revealed, as expected, the thermal expansion of the mullite and alumina phases. However, beginning around 900 °C, the expansion coefficient of the *a*-axis of the mullite crystal structure (the crystal structure being close to tetragonal in the as-received fibre) began to decrease with increasing temperature and subsequently became negative, implying shrinkage of the *a*-axis. The resulting change in axial ratio was largely retained on cooling. At the same time changes in relative peak-intensities indicated an increase in the amount of alumina. These observations suggest the initiation of a permanent change in the fibre involving a reduction in aluminium content in the mullite associated with a shift in crystal structure from near-tetragonal to orthorhombic, an effect reported earlier by Wilson et al.[26]

The Raman spectroscopy indicated no change in the composition of the fibres after heat-treatment for 100 h at 1100 °C. Also the spectra for the matrix were very similar before and after heat-treatment, the only difference detected being a slightly higher content of alumina after heat-treatment. No cristobalite was detected in the matrix or the fibres either before or after heat-treatment.

5. Discussion

The mechanical test results revealed that thermal exposure of the composites at 1000 °C and above caused embrittlement and, in the case of 0/90° composites, loss of strength. This degradation was particularly marked after 100 h at 1100 °C when the 0/90 material exhibited a fracture toughness and notch sensitivity that would be expected of a monolithic ceramic. A number of reasons for such degradation can be sought including: (i) sintering of the matrix leading to reduction in porosity and consequently a loss of the supposed crack deflection behaviour (ii) increased bonding between fibre and matrix leading to a similar effect (iii) strength reduction of the matrix due to phase changes and/or grain growth (iv) degradation of the fibre.

The porosity measurements, supported by microhardness measurements indicated clearly that matrix densification occurred during thermal exposure. The overall shrinkage of the samples was negligible due to the constraint of the continuous fibre skeleton but the shrinkage occurred internally leading to opening of matrix cracks and growth of existing voids. An increased bonding between fibres and matrix also occurred as evidenced by an increased adherence of matrix to the fibres observed on fracture surfaces. Both matrix strengthening and increased fibre/matrix bonding was indicated by the increasing stiffness of the composites. Evidence for a strengthening of the matrix and the fibre/matrix bonding is also provided by the fact that the strength of the ±45 composite, which is dominated by the matrix properties, increased while its strain to failure decreased with thermal exposure. Thus, after 100 h at 1100 °C the 0/90 and ±45 materials had similar mechanical properties approaching the behaviour of a monolithic ceramic.

There were some indications of phase transformation, namely the formation of cristobalite after 100 h at 1100 °C. This was observed by XRD but not by Raman spectroscopy. However, in the latter method spectra were taken from a restricted number of spots in the sample and could therefore have overlooked cristobalite if this existed locally. Phase studies of the alumina–silica (A–S) system show that mullite can exist over a relatively wide range of A:S ratios.[27] The composition of the matrix in the present composites is considered to lie well within this range. However, if the matrix mixture were inhomogeneous, as was indicated by the metallographic studies, regions of high silica content lying outside the mullite range and therefore having a potential for cristobalite formation could have existed locally. An alternative explanation for the occurrence of cristobalite is that the matrix, prepared from an alumina–silica mixture, had not fully reacted to mullite at all places. The formation of mullite matrices in similar composites has been observed to occur via cristoballite formation at temperatures as low as 1240 °C.[28] Cristobalite is generally considered to be a high-temperature form of silica occurring above about 1450 °C [27] but could well be encouraged to form at lower temperatures by the nature of the precursor reactants and/or impurity species such as Na and K.[29] In view of the local and transient nature of cristobalite in the composites it is considered that its formation did not contribute directly to the composite degradation.

Regarding the strength retention of Nextel 720 fibres after thermal exposure, the present authors are not aware of any reported measurements for exposures corresponding to the thermal treatments applied to the composites in this work. However, the HT-XRD results presented here and the few reported results of strength loss of fibres indicate that permanent structural changes can occur in the fibre and that this would be accompanied by some strength loss. Such strength loss could lead to the reduction in fibre pull-out observed on the fracture surfaces but this could equally well be attributed to the increased fibre-matrix bonding. Resolution of this question awaits further studies of fibre strength degradation due to thermal exposure.

6. Conclusions

The effects have been investigated of thermal exposure on the microstructure and stress–strain behaviour

of a woven, continuous oxide fibre reinforced composite with a porous oxide matrix, the stress–strain behaviour being evaluated on centre-hole notched plates.

In the as-received condition the 0/90° orientation of the composite exhibited non-brittle behaviour and moderate notch sensitivity at room temperature, 1000 and 1100 °C. The non-brittle behaviour and low notch sensitivity could be attributed to both extensive fibre-matrix debonding and shear damage in the matrix. The ±45 orientation also had low notch sensitivity. At 1000 °C it exhibited a significantly higher fracture stress and fracture strain than at room temperature. This effect can be attributed to simultaneous sintering and creep of the matrix occurring during the test.

Thermal exposure at 1000 and 1100 °C caused a progressive degradation of the composite indicated, in the 0/90° composite, by a fall in room-temperature strength and strain to failure for a given sample geometry (a/w ratio). This degradation could be described in terms of a Larson–Miller plot which consequently permitted the prediction of the strength loss for a given exposure temperature and time combination within the investigated experimental range. Thermal exposure of the ±45 composite led to an increase in its room-temperature fracture strength but also a marked embrittlement.

The embrittlement of the 0/90° material could be successfully characterised in terms of an effective fracture toughness (K_C) and effective damage zone length (c_0) derived on the basis of the simple model of Waddoups et al.[21] These parameters were constant (i.e. independent of a/w) for a given thermal exposure but decreased consistently with thermal exposure temperature and time.

Exposure for 100 h at 1100 °C led to almost "complete" degradation of the composite in the sense that the fracture was brittle and the values of K_C and c_0 fell to values characteristic for a monolithic oxide while the notch sensitivity was much greater than for the lower thermal exposures. The fact that the ±45 samples exhibited similar stress–strain behaviour after the same exposure is consistent with this interpretation.

Microstructural and fractographic examination indicated that the property degradation was caused by a combination of matrix densification and increased fibre/matrix bonding. Some degradation of fibre properties could also have been a contributory factor. Formation of cristobalite was observed in samples treated for 100 h at 1100 °C. This was deemed to have occurred locally in the matrix and not to have contributed directly to the property degradation.

Acknowledgements

This work was sponsored in part by the US Department of Energy, Assistant Secretary for Energy Efficiency and Renewable Energy under contract DE. AC05-00OR22725 with UT-Battelle, LLC. Financial support from the Swedish Research Council for Engineering Sciences (TFR) is also acknowledged. The authors thank Dr. Michael Lance for performing the RAMAN experiment and Siemens-Westinghouse and Composite Optics for providing the material used in this study. Dr. Oleg Babushkin is acknowledged for performing the XRD experiments.

References

1. Tu, W.-C., Lange, F. F. and Evans, A. G., Concept for a damage-tolerant ceramic composite with "strong" interfaces. *J. Am. Ceram. Soc.*, 1996, **79**, 417–424.
2. Levi, C. G., Yang, J. Y., Dalgleish, B. J., Zok, F. W. and Evans, A. G., Processing and performance of an all-oxide ceramic composite. *J. Am. Ceram. Soc.*, 1998, **81**, 2077–2086.
3. Kelly, A., Zweben, C., ed., *Comprehensive Composite Materials*. Elsevier Science Ltd, London, 2000.
4. Antti, M.-L. and Lara-Curzio, E., Effect of notches, specimen size, and fiber orientation on the monotonic tensile behavior of composites at ambient and elevated temperatures. *Ceram. Eng. Sci. Proc.,* 2001, **22**, 643–650.
5. Turner, K. R., Speck, J. S. and Evans, A. G., Mechanisms of deformation and failure in carbon-matrix composites subject to tensile and shear loading. *J. Am. Ceram. Soc.*, 1995, **78**, 1841–1848.
6. Heredia, F. E., Spearing, S. M., Mackin, T. J., He, M. Y., Evans, A. G., Mosher, P. and Brondsted, P., Notch effects in carbon matrix composites. *J. Am. Ceram. Soc.*, 1994, **77**, 2817–2827.
7. Heredia, F. E., Spearing, S. M., Evans, A. G., Mosher, P. and Curtin, W. A., Mechanical properties of continuous-fiber-reinforced carbon matrix composites and relationships to constituent properties. *J. Am. Ceram. Soc.*, 1992, **75**, 3017–3025.
8. McNulty, J. C., Zok, F. W., Genin, G. M. and Evans, A. G., Notch sensitivity of fiber-reinforced ceramic-matrix composites: effects of inelastic straining and volume-dependent strength. *J. Am. Ceram. Soc.*, 1999, **82**, 1217–1228.
9. Buchanan, D. J., John, R. and Zawada, L. P., Notched fracture behavior of oxide/oxide Nextel™720/AS composite. *Ceram. Eng. Sci. Proc*, 2000, **21**, 581–588.
10. Heathcote, J. A., Gong, X.-Y., Yang, J. Y., Ramamurty, U. and Zok, F. W., In-plane mechanical properties of an all-oxide ceramic composite. *J. Am. Ceram. Soc.*, 1999, **82**, 2721–2730.
11. Kramb, V. A., John, R. and Zawada, L. P., Notched fracture behavior of an oxide/oxide ceramic-matrix composite. *J. Am. Ceram. Soc.*, 1999, **82**, 3087–3096.
12. Mackin, T. J. and Roberts, M. C., Evaluation of damage evolution in ceramic-matrix composites using thermoelastic stress analysis. *J. Am. Ceram. Soc.*, 2000, **83**, 337–343.
13. Jurf, R. A. and Butner, S. C., Advances in oxide–oxide CMC. In: *Proc. Int. Gas Turbine and Aeroengine Congress and Exhibition*, Indianapolis, IN, 1999.
14. Personal Communication with E. Carelli, Siemens Westinghouse, Pittsburgh, PA.
15. Deléglise, F., Berger, M. H., Jeulin, D. and Bunsell, A. R., Microstructural stability and room temperature mechanical properties of the Nextel 720 fibre. *Journal of the European Ceramic Society*, 2001, **21**, 569–580.
16. Milz, C., Goering, J. and Schneider, H., Mechanical and microstructural properties of Nextel™ 720 relating to its suitability for

high temperature application in CMCs. *Ceram. Eng. Sci. Proc*, 1999, **21**, 191–198.
17. Petry, M. D. and Mah, T. I., The effect of thermal exposures on the strengths of Nextel™ 550 and 720 filaments. *J. Am. Ceram. Soc*., 1999, **82**, 2801–2807.
18. Savin, G. N., *Stress Concentrations around Holes*. Pergamion Press, London, 1961.
19. Young, W. C., *Roark's Formulas for Stress and Strain*, 6th ed.. MacGraw-Hill, N.Y, 1989.
20. Tan, S. C., Finite width correction factor for anisotropic plate containing a central opening. *J. Composite Materials*, 1988, **22**, 1080–1097.
21. Waddoups, M. E., Eisenmann, J. R. and Kaminski, B. E., Macroscopic fracture mechanics of advanced composite materials. *J. Composite Materials*, 1971, **5**, 446–454.
22. Whitney, J. M. and Nuismer, R. J., Stress fracture criteria for laminated composites containing stress concentrations. *J. Composite Materials*, 1974, **8**, 253–265.
23. Suo, Z., Ho, S. and Gong, X., Notch ductile-to-brittle transition due to localized inelastic band. *J. Eng. Materials and Technology*, 1993, **115**, 319–326.
24. Babushkin, O., unpublished work.
25. Antti, M.-L., Lara-Curzio, E. and Ferber, M. K., Analysis of damage evolution in continuous fiber-reinforced oxide/oxide composites under cyclic loading, using infra-red thermography. *Ceram. Eng. Sci. Proc*., 2001, **22**, 711–716.
26. Wilson, D. M., Lieder, S. L. and Lueneburg, D. C., Microstructure and high temperature properties of Nextel 720 fibres. *Ceram. Eng. Sci. Proc*, 1995, **16**, 1005–1014.
27. Klug, F. J., Prochazka, S. and Doremus, R. H., Al_2O_3-SiO_2 system in the mullite region. *J. Am. Ceram. Soc*., 1987, **70**, 750–759.
28. Pearce, D. H., Jickells, A. J. and Ponton, C. B., Fabrication of sapphire fibre reinforced ceramic matrix composite. *British Ceram. Trans*, 1996, **95**, 141–145.
29. Stevens, S. J., Hand, R. J. and Sharp, J. H., Polymorphism of silica. *J. Materials Science*, 1997, **32**, 2929–2935.